AIAA JOURNAL
Vol. 32, No. 1, January 1994

Atomic Oxygen Generators for Surface Studies in Low Earth Orbit

Masahito Tagawa,* Masakazu Tomita,† Masataka Umeno,‡ and Nobuo Ohmae§
Osaka University, Osaka 565, Japan

Two facilities for the generation of energetic atomic oxygen beams have been developed to investigate the degradation of materials in low Earth orbit. An atomic oxygen generator using an ion beam method was used mainly for studying the effect of kinetic energies on surface reactions. Another generator combined pulsed supersonic valve and pulsed YAG laser systems for long-duration exposure experiments without maintenance. The velocity of atomic oxygen was measured by a retarding energy analyzer and a plasma time-of-flight analyzer. Increments of mass in silver films due to the formation of oxides show that the fluxes of atomic oxygen exceed $10^{12} \sim 10^{13}$ atoms/cm^2 s. X-ray photoelectron spectroscopy spectra of O1s on a single MoS_2 crystal exposed to energetic atomic oxygen showed the existence of energy dependence of the surface reaction.

Introduction

MATERIAL degradation in low Earth orbit (LEO) is one of the most serious problems for large structures which will operate in LEO for a long duration. To maintain the function of mechanical, electronic, and thermal systems facing in the ram direction, an evaluation of systems damage caused by the attack of atomic oxygen (AO) having 5 eV kinetic energy (8 km/s) is necessary.[1-7] In ground-based facilities it is quite difficult both to produce a relative kinetic energy of 5 eV and to exceed the flux of 10^{13} atoms/cm^2 s in LEO at the same time. Therefore, two alternative approaches should be considered to evaluate the material degradation in LEO. One approach is to estimate the quantitative degradation of materials from the mechanism of the reaction. The type of facility required to do this does not need an extremely large flux such as those used for accelerated testing, but rather a high-quality AO beam, i.e., kinetic energy of 5 eV. Analytical results of exposed surfaces with surface-sensitive analyses determine the reaction in LEO and predict the reaction efficiency, degree of degradation, and damage to systems. An AO generator which satisfies the technical properties described earlier is based on the ion beam technique that can obtain high-purity AO beams with the correct energy and a small full width at half-maximum (FWHM). Both positive and negative ion beams have been used for this kind of AO generator. Electron attachment or the charge transfer technique are used to neutralize the positive ion beam,[8,9] whereas the photodetachment technique is applied to a negative beam.[10-12] The other approach works from the opposite standpoint of the ion beam method, i.e., quantitative degradation of materials is examined by accelerated testing without sufficient kinetic energy of AO. The data base constructed by this approach must be equipped with sufficient safety factors when selecting materials for space application. Conventional plasma asher facilities or rf/microwave plasma systems are used for this approach.[13-18] However, these experiments will provide neither engineering data on the reliability of the system nor on the reaction efficiencies in LEO. This is because there is no evidence that the reactions in LEO are accurately simulated in chambers on the ground. Therefore, it is necessary, when evaluating the material degradation of materials in LEO, to combine these two approaches or to make a brand new facility which can realize all of these requirements. Such a new facility was pioneered by Caledonia and Krech[19] at Physical Science Inc. (PSI). Using a pulsed valve and pulsed CO_2 laser, they obtained energies ranging from $2 \sim 13$ eV and fluxes of $\sim 10^{16}$ atoms/cm^2 s (see Refs. 19–22). Cross and Cremers[23] and Cross et al.[24] also developed an AO generator with a continuous wave CO_2 laser and a supersonic nozzle system. This generator realized the energies of about ~ 2 eV and flux of 10^{16} atoms/cm^2 s. These facilities are categorized in laser-induced breakdown methods and appear to satisfy, in part, the requirements discussed here.

In this research, two AO generators, based on an ion-beam method and a laser-induced breakdown, were developed. The ion-beam-type AO generator was especially designed for obtaining a well-defined, pure AO beam with a small FWHM of the beam energy. The laser-breakdown-type AO generator combined a pulsed supersonic valve and a YAG laser. The basic configuration of the facility was similar to PSI's, however, an optical detonation wave was not utilized for accelerating the AO. Thus, the laser-breakdown AO generator developed in this study is located in an intermediate position between the two laser-induced-breakdown AO generators described earlier. Diagnostics of the AO beam generated with these facilities, as well as surface reactions with AO, were studied.

Atomic Oxygen Generators

Ion-Beam-Type Atomic Oxygen Generator

Figure 1 schematically presents the ion-beam AO generator developed in this study. A Penning ionization gauge (PIG) ion source, which has been known as an electron impact ionization source, was chosen as an oxygen plasma producer. The reason for choosing this type of ionization source is that an ion beam which has a small FWHM of a beam energy is

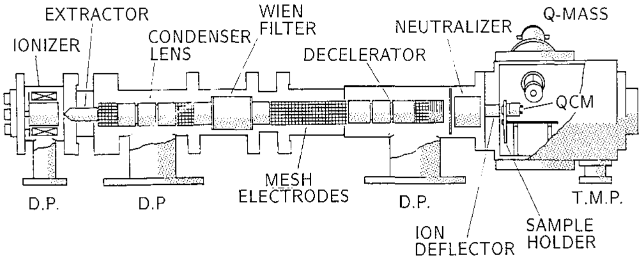

Fig. 1 Schematic drawing of the ion-beam-type atomic oxygen generator.

Received July 28, 1992; revision received May 25, 1993; accepted for publication May 26, 1993. Copyright © 1993 by the American Institute of Aeronautics and Astronautics, Inc. All rights reserved.

*Research Associate, Department of Precision Engineering, 2-1 Yamadaoka, Suita. Member AIAA.

†Graduate Student, Department of Precision Engineering, 2-1 Yamadaoka, Suita.

‡Professor, Department of Precision Engineering, 2-1 Yamadaoka, Suita.

§Associate Professor, Department of Precision Engineering, 2-1 Yamadaoka, Suita.

obtained, although the lifetime of its W filament is not long enough in the oxygen plasma. To compensate for this shortcoming, multiple W filaments were placed in the ion source. The exchange of W filaments was managed by switching the terminal without causing the vacuum to leak. The PIG ion source was operated at a typical discharge voltage of 60 V with an oxygen pressure of 10^{-3} Torr. A discharge current of more than 700 mA was obtained under these experimental conditions. To avoid inflow of the oxygen gas downstream of the facility, the ion source chamber is evacuated by an independent vacuum pumping system with a sufficient pumping speed. Oxygen ions generated in oxygen plasma are extracted with the single hole extraction system, the hole diameter being 1 mm. The divergence of the oxygen beam is about 7 deg, and the beam was focused by the condenser lenses located next to the extraction electrode. The condenser lens consists of three electrodes whose diameter is 40 mm. Voltages of the first and the third electrodes are -900 V, which is the same voltage as the extraction voltage, and that of the second electrode is typically kept at -270 V. Impurity ions contained in the oxygen beam are eliminated with a mass filter. A high transmittance and small size are required for the mass filter used in this facility, rather than a high resolution of mass/charge ratio. Thus, a Wien filter 6 cm in length was inserted in the beam line. Magnetic shields with permalloy were attached to both sides of the filter to minimize the influence of leakage of the magnetic field from the Wien filter. The Wien filter also has a role as a bandpass velocity filter. This contributes to the realization of the oxygen ion beam with a small FWHM. Thus, the pure O_2^+ beam enters the deceleration lens consisting of 13 electrodes. This type of decelerator is called a chemical accelerator,[25] and the voltage of each electrode is determined experimentally. The neutralization of oxygen ions was carried out using the decomposition-recombination reaction of oxygen ions under the effect of electrons. The high reaction rate of this combination is known by the chemical reaction

$$O_2^+ + e^- \Longleftrightarrow O_2^* \Rightarrow 2O \qquad (1)$$

In accordance with this reaction, the discharge condition of oxygen at the PIG ion source has been determined experimentally to produce as many O_2^+ ions as possible. Residual oxygen ions remaining after neutralization were eliminated by an ion deflector placed in front of the samples. Samples were mounted on the sample holder which can be rotated along the beam axis. A Faraday cup and viewing hole were equipped on the holder to measure the beam current and to keep the axis of the facility straight. The length of the facility is about 1.5 m. The chamber is evacuated with a differential pumping system consisting of three oil diffusion pumps and one turbo molecular pump. The vacuum level is maintained on the order of 10^{-7} Torr in the beam line, and 10^{-8} Torr in the reaction chamber under operational conditions.

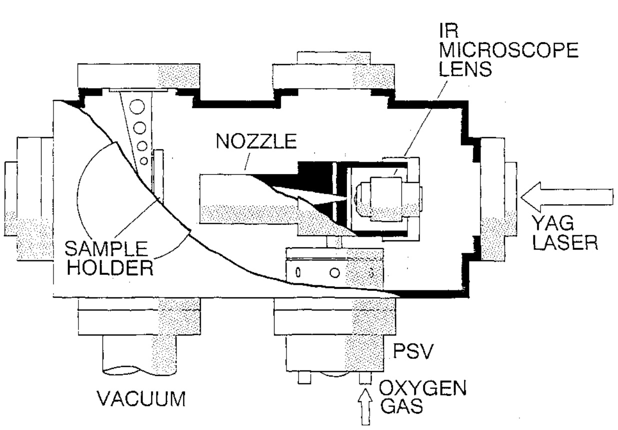

Fig. 2 Schematic drawing of the atomic oxygen generator based on laser-induced breakdown of oxygen.

Laser-Breakdown-Type Atomic Oxygen Generator

Figure 2 schematically presents the laser-breakdown-type AO generator developed in this study. A pulsed supersonic valve (PSV) is attached to the bottom of the vacuum chamber (300 × 300 × 700 mm) which is evacuated by a turbo molecular pump with a pumping speed of 340 l/s. The ultimate vacuum pressure of this chamber is 10^{-9} Torr, however, the vacuum falls instantly to 10^{-4} Torr when oxygen gas is introduced at 0.2 Hz. Oxygen gas is introduced to the nozzle throat through the PSV. The plenum pressure of the PSV is kept at 12 atm. A YAG laser is flashed from the backside of the nozzle through a quartz window. This configuration allows a large effective exposure area for the sample, since there is no need to locate a laser aperture on a sample stage as there is in the PSI system. Moreover, a high-magnification IR lens with a short focal length generates laser-induced breakdown even with use of a relatively low-power laser (25 mJ/pulse). The plasma front generated by the laser breakdown moves opposite to the samples at a velocity of the order of 100 km/s (see Ref. 26). The AO generator developed at PSI utilizes this plasma front and optical detonation waves, which moved in the sample direction, for decomposition and acceleration of the oxygen molecules and atoms. However, the moving direction of the plasma front and the strong detonation waves in this facility are opposite to the samples because of the direction of laser irradiation. This configuration allows us to avoid the unexpected effects of strong shock waves on the samples. Since laser flash time is quite short compared with the PSV operation time, a lot of surplus oxygen gas exists around the breakdown point. This means that fast AO generated in the plasma collides with surplus oxygen molecules, mainly at the forward region of the nozzle. As a result, AO recombines to molecular oxygen (MO). To avoid this recombination, the almost-surplus oxygen gas introduced before the laser flash should be exhausted through the bypass line. The focal point of the laser in the cross section of gas flow is also important for obtaining an AO beam with the correct energy. The focal point was set at a periphery of the flow where the following conditions are satisfied: 1) a sufficient amount of MO exists at the focal point, and 2) accumulated MO exists between the focal point and the edge of the flow. The former condition relates to the condition of the lower boundary of oxygen pressure at which laser-induced breakdown could ocuur. The latter condition is due to the deceleration of the AO velocity from 30 to 5 eV. The velocity of the beam strongly depends on the focal point of the laser. A precise adjustment of the collimation of the laser beam and of the laser flash timing are thus necessary. A dimension of the whole system including vacuum pumps is within 1 × 1 × 1 m, so that it is easy to combine the other facility to make in-situ studies of the degradation of materials.

Diagnostic of the Beam

Velocity of the Beam

One of the most important parameters accounting for the reaction with AO in LEO is its kinetic energy. The kinetic energy of an AO beam generated by the ion-beam-type AO generator depends on a potential difference between the plasma in the ionizer and the plasma in the neutralizer. It is known that the plasma potential of the PIG ionizer is correlated with the anode potential of the ion source. Therefore, to estimate the energy distribution of the atomic oxygen beam, the kinetic energy of the oxygen ion beam and space potential in the neutralizer must be measured. The total energy distribution (TED) of oxygen ions obtained in this facility was measured by using a modified van Oostrom energy analyzer.[27] This energy analyzer is a type of retarding potential analyzer, so that a differentiation procedure is required to obtain the TED spectra. An image processing system was used for differentiating the spectra digitally. The TEDs of oxygen ions thus obtained are indicated in Fig. 3. It is clear from Fig. 3 that the peak energy of the oxygen ion beam is almost the same as the

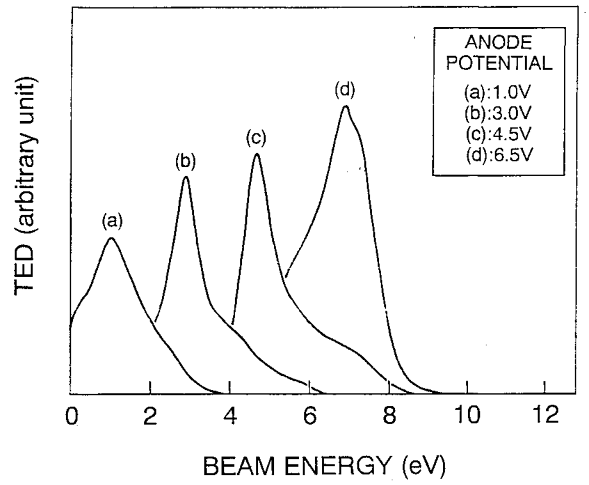

Fig. 3 Total energy distribution of oxygen ions measured by the modified van Oostrom energy analyzer.

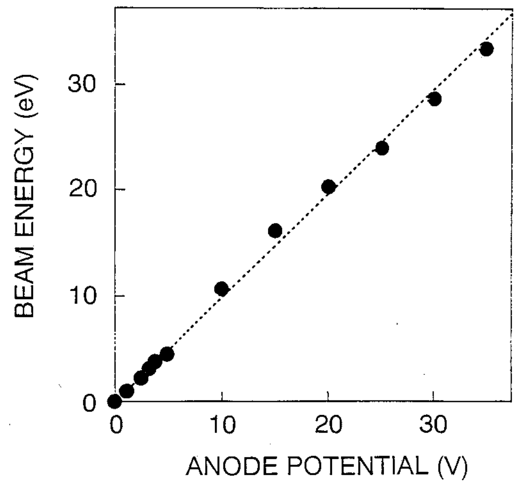

Fig. 4 Linear relation between the anode voltages in the PIG ion source and beam energies.

anode potential. The peak energies are replotted in Fig. 4 against the anode potential. From this relationship the beam energy can easily be adjusted by changing the anode potential of the ion source. The FWHM of the spectrum was only 1.1 eV at the kinetic energy of 5 eV. This value is the smallest in the AO generators attained until now; FWHMs of 15, 3.5, and 4.2 eV were reported in previous papers.[28-30] The FWHM of AO in LEO is considered to be 2 eV,[31] so that the FWHM value seems to be small enough to study an energy dependence of the reaction with AO in LEO.

The energy distributions measured in Fig. 3 were not for AO but for oxygen ions before they neutralized. There is a possibility that the beam energy will be changed by the neutralization. However, in the case of neutralization by means of electron attachment, momentum transfer in the reaction is negligibly small compared to a charge transfer reaction with H_2O molecules. Therefore, the influence of neutralization on the velocity of the AO beam will not be large. In contrast, since this reaction is exothermionic, the internal energy of AO generated by this reaction may become high. Specifically, AO in metastable states can be generated. The content of metastables in the beam has not been studied yet. However, the measurement of metastables will be needed to discuss the surface reaction of the beam generated in this apparatus.

The TED spectra indicated in Fig. 3 were measured with respect to a ground potential. The kinetic energy of AO will be shifted by the voltage difference between a space potential in the neutralizer and the ground potential, because after the neutralization the electric potentials do not work on neutral species. This is the reason why the space potential in the neutralizer must be measured precisely. Space potential as well as electron density in the neutralizer were measured by means of the Langmuir probe method. The neutralizer consists of a tungsten filament, inner mesh electrode, and outer electrode. The electrons emitted from the filament were accelerated by the potential difference between the filament and the inner mesh electrode, and stored on the axis. Potentials both at the outer electrode and at the filament of the neutralizer are adjustable, whereas the inner electrode is held at a ground potential to keep the space potential in the axis close to the ground potential. It becomes clear that the space potential in the neutralizer exceeds -20 V when the voltages applied to the outer electrode and the filament become negatively high. However, the electron density does not increase in this case. The efficiency of neutralization becomes high with increasing the electron density. The filament and the outer electrode voltages were set at -10 and -4.5 V, respectively, so as to give a low space potential (-5 V) with high electron density ($10^{13}/m^3$).

It is usually difficult to measure the velocity of neutral species. A new technique for measuring the velocity of a pulsed AO beam generated by the laser-breakdown-type apparatus was also designed. The measuring technique is based on the glow of discharged gases and was therefore named as the plasma time-of-flight (TOF) measurement. The essentials of plasma TOF are shown in Fig. 5. A high-voltage wire was located in front of the nozzle as shown in Fig. 5. High voltage, up to 2 kV, was typically applied to the wire. Only when a

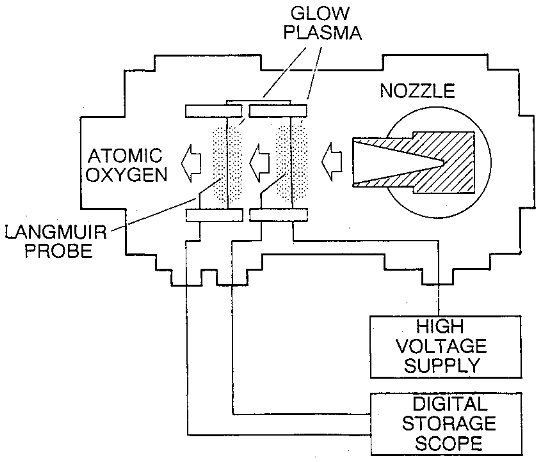

Fig. 5 Schematics of the plasma time of flight (TOF) measurement.

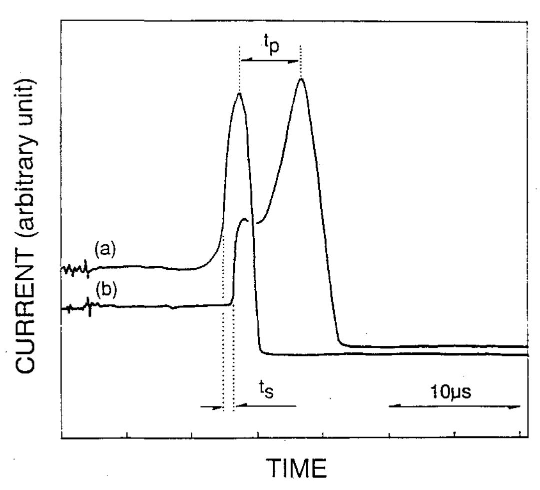

Fig. 6 Plasma TOF diagram of atomic oxygen beam obtained at (a) 15 mm and (b) 25 mm downstream from the nozzle.

pulsed AO beam came to the wire glow discharge occurred around the wire. Ions and electrons thus generated in the glow discharge were detected by the Langmuir probe located near the high-voltage wire. By moving this equipment along the beam axis, discharge phenomena at all locations were recorded by a digital storage oscilloscope. Since the conditions of glow discharge are strongly dependent on the gas pressure, the time difference was detected when the same condition of discharge occurs in each position of the equipment. From the time difference of the discharge and the distance between the positions of this equipment, one can calculate the velocity of AO.

Figure 6 indicates the time-of-flight diagrams of a fast AO beam obtained in this apparatus. In Fig. 6, (a) and (b) correspond to the diagrams recorded at 15 and 25 mm downstream, measured from the end of the nozzle. In (a), only one peak is visible. However, one can find two peaks in (b). The small peak in (b) is due to a fast AO beam accelerated by laser breakdown, and the large peak is produced by the nonaccelerated AO. It is difficult to distinguish two peaks in the case of (a). The velocities of accelerated and nonaccelerated AO and MO were measured by the time differences in the threshold and the time differences in the main peaks of (a) and (b). The time differences between the threshold and the main peaks in the diagram, i.e., Δt_s and Δt_p, are 0.87 and 3.5 μs, and these correspond to 11.6 km/s (10 eV) and 2.9 km/s (0.6 eV), respectively. The results in Fig. 6 suggest that the velocity of the AO beam distributes from 2.9 to ~ 11.6 km/s, i.e., from 0.6 to ~ 10 eV, in these experimental conditions. The velocity of the beam is varied by changing the laser-flash timing. Figure 7 indicates the relationship between the delay time of the laser flash and the energy of AO calculated from Δt_s. This figure shows that the velocity of the AO beam is adjustable from 0.6 to 20 km/s by changing the laser-flash timing.

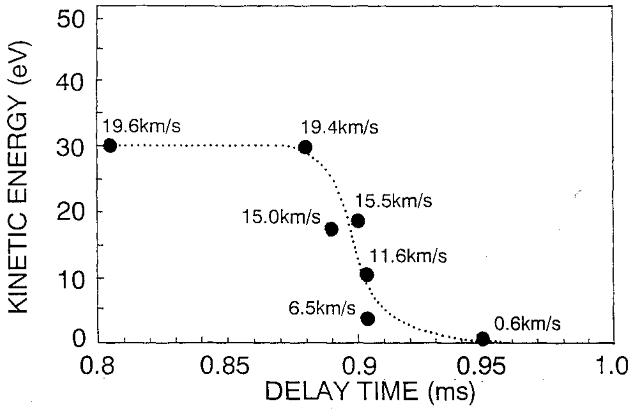

Fig. 7 Relation between the delay time of the laser flash and kinetic energies of atomic oxygen beam.

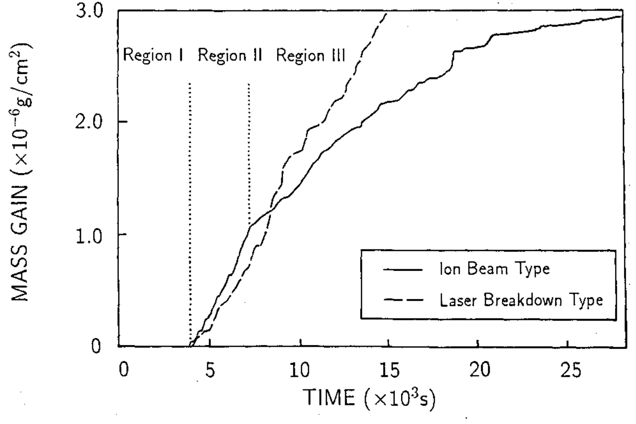

Fig. 8 Mass increment of the silver film due to the exposure to atomic oxygen beam.

Table 1 Comparison of the results in the XPS analyses with various kinetic energies of atomic oxygen beam generated by the ion-beam method and the laser-breakdown method

		Exposed			
	Unexposed	2 eV	5 eV	50 eV	Pulsed laser
Mo	26–31	31	29	36	45
S	69–74	48	54	56	29
O	0	21	17	8	26
S/Mo	2.2–2.8	1.6	1.8	1.5	0.7
O/Mo	0	0.7	0.6	0.2	0.6

Fluxes of the Atomic Oxygen Beam

Direct measurement of flux of the AO was performed by using a quartz crystal microbalance (QCM) with silver electrodes proposed by Matijasevic et al.[32] This method is based on the different reactivity of silver with MO and AO, i.e., silver is not oxidized by MO but is oxidized by AO. The mass increase due to the oxidation of silver by AO is detected with the QCM. The QCM used in this study was a standard AT cut, 5 MHz Sloan crystal. The QCM was attached to the rotatable sample holder on the beam axis. Stability of the resonance frequency of the QCM was confirmed during an aging treatment over several hours. The frequency was measured at every 10 s. After exposure, the silver surface was analyzed by X-ray photoelectron spectroscopy (XPS) to identify the concentration of Ag and O. XPS measurements did not indicate notable contaminations. Change in the mass Δm due to oxidation was calculated from the frequency shift of the QCM by the relation of

$$\Delta f = f_0^2 \Delta m/(NA\rho) \qquad (2)$$

where f_0 is the initial resonance frequency, ρ the density of quartz, A the frequency constant, and Δf the shift in the resonant frequency. Changes in the mass of silver films during exposure were plotted in Fig. 8. The solid and broken lines indicate mass increments of silver films by using an ion-beam-type and a laser-breakdown-type AO generator, respectively. In the case of the AO beam obtained by the ion-beam-type AO generator, the entire system of the generator was operative, at first, except for potential of one electrode of the decelerator, and consequently oxygen ions could not reach the neutralizer. Under this experimental condition, the frequency of the QCM stabilized to a certain value (region I of Fig. 8). After the application of the correct potential to the electrode, an increment of increased mass was observed. Initially, the mass increased linearly with the exposure (region II), and after a certain exposure time it increased with a square root of the exposure (region III). This phenomenon is widely known as the linear-parabolic law of oxidation.[33] The initial linear behavior was governed by the sticking or the reaction of AO on the silver film, and the latter behavior by the diffusion process of either AO or silver atoms in the oxide film. From the slope of the initial linear mass increase in region II, a lower bound of the AO flux could be estimated, assuming that the sticking coefficient of AO on silver surface is unity. The lower bound for the flux of 5 eV of AO generated in this generator was calculated to be about 1×10^{13} atom/cm^2 s, which corresponds to the flux of AO in LEO at an altitude of 500 km.

In contrast, in the laser-breakdown-type AO generator case (broken line in Fig. 8), the flux of AO was calculated to be 1.7×10^{12} atoms/cm^2 s. This value is one-tenth of that in LEO, and much smaller than that obtained by the other AO generators reported in Refs. 19–24. However, the present experimental work was done at an operating frequency of 0.2 Hz, and this problem will be solved by simply increasing the laser repetition rate and the pumping speed of the chamber.

Reaction of MoS_2 with Energetic Atomic Oxygen

Molybdenum disulfide (MoS_2) is one of the most important materials for space tribology.[34] Since surface properties play a major role in tribology, it has been assumed that the AO has serious influences on the tribological properties of MoS_2. However, the change in properties of MoS_2 due to its exposure to energetic AO has remained unclear. Therefore, an AO beam with kinetic energies of 2, 5, and 50 eV was exposed to the (0001) surface of a single crystal of MoS_2. Single crystals of MoS_2 were also exposed to a 5 eV AO beam generated by a laser-breakdown-type AO generator. Fluence for each sample is 3.5×10^{17} atoms/cm^2, which corresponds to 9 h of exposure in LEO at 500 km. Experiments were carried out at room temperature. After exposure the surfaces were analyzed by XPS (Perkin Elmer ESCA-5000LS spectrometer). The results obtained by the XPS analyses are summarized in Table 1. Since the (0001) MoS_2 surface is chemically inactive, adsorbed oxygen cannot be detected before exposure. However, the existence of oxygen at the surface is detected after exposure at all energy ranges. Moreover, it is clearly observed that the higher the kinetic energy, the lower the atomic concentration of oxygen becomes. This suggests that the behavior of AO at the surface is kinetic energy dependent. The reasons for this phenomenon are considered to be the following: 1) The sticking coefficient of AO on MoS_2 depends on its kinetic energy. Namely, the higher the kinetic energy is, the lower the sticking coefficient becomes. 2) Sputtering of SOx and/or O atoms occurs at the surface of MoS_2 when the kinetic energy of AO becomes higher. Both of these reasons are believed to contribute to the results. The S/Mo ratios listed in Table 1 are nearly constant (1.5–1.8) after the exposures, although they are reduced compared to the ratio before exposure (2.2–2.8), which indicates that the reaction of gasification of sulfur as SOx occurs at every kinetic energy level. This result was also identified by the quadrupole mass analyzer equipped at the reaction chamber. Namely, enhanced peaks of $m/e = 48$ and 64, corresponding to SO and SO_2, were detected during exposure.[35]

The oxygen concentration of the MoS_2 surface exposed to the AO beam generated by the laser-breakdown-type AO generator (26%) is higher than that generated by the 2 eV AO beam generated by the ion beam apparatus (21%) as shown in Table 1. This fact implies that the formation of reaction products on the MoS_2 surface was induced mainly by the AO with energies lower than 2 eV, even in the case where the laser breakdown apparatus was used. This result agrees with the velocity distribution of the AO beam obtained from Fig. 5, i.e., the AO beam generated by this facility involves a great amount of low energetic AO and MO. The high concentration of oxygen at the surface suggests that there are no influences of the high-energy particles or shock waves which may be generated in a laser-induced breakdown. One of the most significant points of the results obtained in this facility is the low surface concentration of sulfur (26%) and low S/Mo ratio (0.7). The normalized oxygen concentration obtained in this facility (O/Mo ratio) shows almost the same value (0.6) as those of 2 or 5 eV AO beams generated by the ion-beam-type AO generator. The sputtering effect for Mo is less significant than it is for S, and Mo does not show gasification after oxidation. Thus, this result is interpreted that the absolute amount of oxygen atoms on the MoS_2 surface exposed to AO by the laser-breakdown AO generator is almost same as it is in the 2 or 5 eV cases. The small S/Mo value of this work, therefore, results from the decrease in the amount of sulfur. It was found that SOx was formed when AO attacked the MoS_2 surface as mentioned earlier. Gasification of SOx leads to the loss of sulfur content at the surface. The fact that a large amount of sulfur reacted at the surface in the case of this facility, even at the same fluences of AO, indicates that the AO generated by the laser-breakdown-type AO generator has a higher reaction efficiency compared with that achieved by ion-beam method.

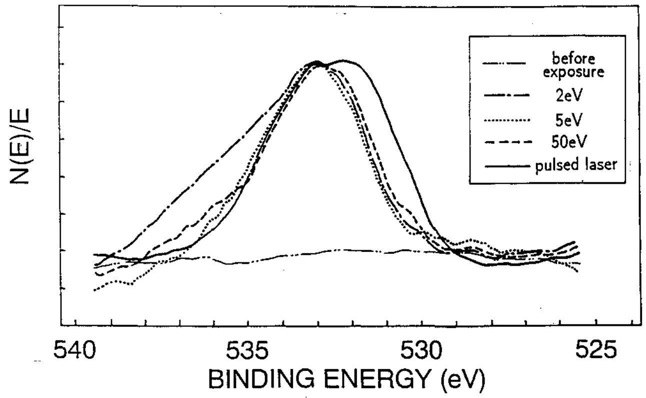

Fig. 9 O1s XPS spectra of the (0001) MoS_2 surfaces before and after exposures to 2, 5, and 50 eV atomic oxygen beams generated by the ion-beam-type and laser-breakdown-type AO generators.

Figure 9 shows O1s peaks obtained from the samples exposed to 2, 5, and 50 eV AO beams obtained by the ion-beam-type facility and one 5 eV AO beam generated by the laser-breakdown-type facility. The peak height of each spectrum is normalized. Each spectrum provides a 533.0 eV oxygen peak due to the exposure of AO. This peak is characteristic of SOx, and it is clear that the oxygen at the surface of the MoS_2 exists as a complex with sulfur. By comparing the three spectra in Fig. 9, i.e., the 2, 5, and 50 eV AO generated by ion-beam-type AO generator, one finds that the spectrum has a tail in the high-binding energy area in the case of MoS_2 exposed to 2 eV AO. This implies that a different binding state exists in the case of AO with a kinetic energy of 2 eV. The origin of the tail near 536 ~ 538 eV is unknown. However, this preliminary results strongly suggest that there is an appropriate energy range for the certain reaction of AO to MoS_2. The same sulfur oxides were formed in the case of 5 and 50 eV beams of the ion-beam method. As for the sample exposed to AO generated by the laser-breakdown-type facility, in spite of the existence of low-energy AO (≤ 2 eV) and MO, it was confirmed that the same sulfur oxides which were formed by the ion-beam method with 5 eV were formed. Molybdenum oxide, which should appear at around 529 eV was not detected in the three samples exposed to AO by the ion-beam facility, so it is assumed that the preferential oxidation of sulfur occurs on (0001) MoS_2 surface by AO. However, the shoulder appearing at 531 eV which can be seen only at the laser-breakdown-type facility is due to molybdenum oxides. The formation of molybdenum oxides also was confirmed for this sample at the Mo 3d XPS spectrum. Thus, it became clear that molybdenum oxides were formed only in the case of the laser-breakdown-type facility. The reaction of AO to single-crystal MoS_2 was reported by Cross et al.[36] and by Arita et al.[37] Cross reported that 45% and 15% of the near-surface Mo atoms were converted into MoO_3 and MoO_2, respectively. In contrast, Arita et al.[37] analyzed AO-exposed samples exposed to AO at PSI. They concluded that Mo atoms on the basal planes of single-crystal MoS_2 were hardly oxidized by AO, whereas those of sputtered MoS_2 were easily oxidized. This difference may not be due to the differences in the translational energies of the AO beams generated by these facilities, i.e., AO with lower translational energy shows higher reactivity. In fact, reactivities of AO generated by the AO generators developed in this study seem to be different even at the same kinetic energy. Therefore, there is a possibility that the differences of these O1s XPS spectra indicated in Fig. 9 are due to either the existence of undecomposed MO or to the differences of electronic states of AO. However, an identification of AO states generated by these two facilities has not been carried out yet, and further diagnostics are also necessary.

Conclusions

Two facilities for the generation of energetic AO beams were developed to investigate the degradation of materials in LEO. One facility is based on an ion-beam technique and the other on a laser breakdown of oxygen gas. Kinetic energy of the AO beam obtained by the ion-beam-type facility can be varied over a wide range, and its FWHM is about 1.1 eV. The kinetic energy of the AO beam obtained by the laser-breakdown-type facility was measured by a plasma TOF system that was specially developed for this research, and the results indicated that the velocity of the AO beam ranged from 0.6 to 10 eV. The increments of mass in silver films due to the formation of oxides shows that the AO were generated and that the flux exceeded $10^{12} \sim 10^{13}$ atoms/cm^2 s, which nearly corresponds to that found in LEO at 500 km. XPS spectra indicate that oxygen with different binding states exists in the case of AO exposure at 2 eV, with almost the same SOx peak found at both 5 and 50 eV. Sulfur oxides formed on the (0001) MoS$_2$ surface by the laser-breakdown-type AO generator show resemblance to those obtained by a 5-eV AO beam generated by the ion-beam-type facility.

Acknowledgments

This study was supported in part by the Grant-in-Aid for Scientific Research (B) 02452112 and 02750052, from the Ministry of Education, Science, and Culture, Japan. The authors are indebted to M. Arita, K. Kishi, and Y. Yasuda of Nissan Motor Co. Ltd. for their helpful discussion and technical support. The authors also thank H. Hara of Kubota Ltd. for the XPS analysis. Appreciation is also expressed to N. Yasu and Y. Ohira for their technical assistance during the experiments.

References

[1] Green, B. D., Caledonia, G. E., and Wilkerson, T. D., "The Shuttle Environment: Gases, Particles, and Glow," *Journal of Spacecraft and Rockets*, Vol. 22, No. 5, 1985, pp. 500–511.

[2] Garrett, H. B., Chutjian, A., and Gabriel, S., "Space Vehicle Glow and Its Impact on Spacecraft Systems," *Journal of Spacecraft and Rockets*, Vol. 25, No. 5, 1988, pp. 321–340.

[3] Peters, P. N., Linton, R. C., and Miller, E. R., "Results of Apparent Atomic Oxygen Reactions on Ag, C, and Os Exposed during the Shuttle STS-4 Orbits," *Geophyscal Research Letters*, Vol. 10, No. 7, 1983, pp. 569–571.

[4] Leger, L. J., "Oxygen Atom Reaction with Shuttle Materials at Orbital Altitude—Data and Experiment Status," AIAA Paper 83-0073, Jan. 1983.

[5] Zimcik, D. G., and Maag, C. R., "Results of Apparent Atomic Oxygen Reactions with Spacecraft Materials during Shuttle Flight STS-41G," *Journal of Spacecraft and Rockets*, Vol. 25, No. 2, 1988, pp. 162–168.

[6] Leger, L. J., Visentine, J. T., and Schliesing, J. A., "A Consideration of Atomic Oxygen Interactions with Space Station," AIAA Paper 85-0476, Jan. 1985.

[7] Whitaker, A. F., Little, S. A., Harwell, R. J., Griner, D. B., DeHaye, R. F., and Fromhold, A. T., Jr., "Orbital Atomic Oxygen Effects on Thermal Control and Optical Materials—STS-8 Results," AIAA Paper 85-0416, Jan. 1985.

[8] Banks, B. A., Rutledge, S., Brdar, M., Olen, C., and Stidham, C., "Neutral Atomic Oxygen Beam Produced by Ion Charge Exchange for Low Earth Orbital Simulation," *Proceedings of the NASA Workshop on Atomic Oxygen Effects*, Jet Propulsion Lab., JPL Pub. 87-14, June 1987, Pasadena, CA, pp. 127–134.

[9] Sjolander, G. W., and Bareiss, L. E., "Martin Marietta Atomic Oxygen Beam Facility," *Proceedings of the 18th International SAMPE Technical Conference* (Covina, CA), Society for the Advancement of Material and Process, May 1986, pp. 722–731.

[10] Orient, O. J., Chutjian, A., and Murad, E., "Reaction and Electronic Excitation in Crossed-Beams Collisions of Low-Energy O(3P) Atoms with H$_2$O and CO$_2$," *Physical Review Letters*, Vol. 65, No. 19, 1990, pp. 2359–2361.

[11] Orient, O. J., Martus, K. E., Chutjian, A., and Murad, E., "Optical Emission Generated by Collisions of 5eV O(3P) Atoms with Surface-Adsorbed Hydrazine," *Journal of Chemical Physics*, Vol. 97, No. 6, 1992, pp. 4111–4114.

[12] Orient, O. J., Martus, K. E., Chutjian, A., and Murad, E., "Recombination of 5-eV O(3P) Atoms with Surface-Adsorbed NO: Spectra and Their Dependence on Surface Material and Temperature," *Physical Review A*, Vol. 45, No. 5, 1992, pp. 2998–3003.

[13] Gulino, D. A., Egger, R. A., and Banholzer, W. F., "Oxidation-resistant Reflective Surfaces for Solar Dynamic Power Generation in Near Earth Orbit," *Journal of Vacuum Science and Technology*, Vol. A5, No. 4, 1987, pp. 2737–2741.

[14] Golub, M. A., and Wyderen, T., "Reaction of Atomic Oxygen (O(3P)) with Various Polymer Films," *Polymer Degradation and Stability*, Vol. 22, No. 4, 1988, pp. 325–338.

[15] Koontz, S. L., Albyn, K., and Leger, L. J., "Atomic Oxygen Testing with Thermal Atom Systems: A Critical Evaluation," *Journal of Spacecraft and Rockets*, Vol. 28, No. 3, 1991, pp. 315–323.

[16] Golub, M. A., Wyderen, T., and Cormia, R. D., "ESCA Study of Kapton Exposed to Atomic Oxygen in Low Earth Orbit or Downstream from a Radio-Frequency Oxygen Plasma," *Polymer Communications*, Vol. 29, No. 10, 1988, pp. 285–288.

[17] Golub, M. A., and Cormia, R. D., "ESCA Study of Poly (Vinylidene Fluoride), Tetrafluoroethylene-Ethylene Copolymer and Polyethylene Exposed to Atomic Oxygen," *Polymer*, Vol. 30, No. 9, 1989, pp. 1576–1581.

[18] Sanders, J. H., and Tatarchuk, B. J., "Pinhole Plugging Characteristics of Silica/Iron/Silver Protective Coatings in Atomic Oxygen Environments," *Thin Solid Films*, Vol. 192, No. 1, 1990, pp. 79–95.

[19] Caledonia, G. E., and Krech, R. H., "Energetic Oxygen Atom Material Degradation Studies," AIAA Paper 87-0105, Jan. 1987.

[20] Caledonia, G. E., Krech, R. H., and Green, B. D., "A High Flux Source of Energetic Oxygen Atoms for Material Degradation Studies," *AIAA Journal*, Vol. 25, No. 1, 1987, pp. 59–63.

[21] Caledonia, G. E., Gauthier, M. J., and Krech, R. H., "High Velocity Atomic Oxygen/Surface Accomodation Studies," AIAA Paper 91-1339, June 1991.

[22] Caledonia, G. E., Krech, R. H., Upschulte, B. L., Sonnenfroh, D. M., Oakes, D., and Holtzclaw, K. W., "Fast Oxygen Atom Facility for Studies Related to Low Earth Orbit Activity," AIAA Paper 92-3974, July 1992.

[23] Cross, J. B., and Cremers, D. A., "Atomic Oxygen Surface Interactions—Mechanistic Study Using Ground-Based Facilities," AIAA Paper 85-0473, Jan. 1985.

[24] Cross, J. B., Spangler, L. H., Hoffbauer, M. A., and Archuleta, F. A., "High Intensity 5eV CW Laser Sustained O-Atom Exposure Facility for Material Degradation Studies," *Proceedings of the 18th International SAMPE Technical Conference* (Covina, CA), Society for the Advancement of Material and Process, May 1986, pp. 740–751.

[25] Herman, Z., Kerstetter, J. D., Rose, T. L., and Wolfgang, R., "A Crossed-Beam Apparatus for Investigation of Ion-Molecular Reactions," *Review of Scientific Instruments*, Vol. 40, No. 4, 1969, pp. 538–544.

[26] Raizer, Y. P., "Laser-induced Discharge Phenomena," *Studies in Soviet Science*, Consultants Bureau, New York, 1977, pp. 180–272.

[27] Tagawa, M., Takenobu, S., Ohmae, N., and Umeno, M., "Electric Field Distribution of Electron Emitter Surfaces," *Applied Physics Letters*, Vol. 50, No. 9, 1987, pp. 545–546.

[28] Outlaw, R. A., Peregoy, W. K., Hoflund, G. B., and Corallo, G. R., "Electron Stimulated Desorption of Atomic Oxygen from Silver," NASA TP-2668, April 1987.

[29] Singh, B., Amore, L. J., Saylor, W., and Racette G., "Laboratory Simulation of Low Earth Orbital Atomic Oxygen Interaction with Spacecraft Surfaces," AIAA Paper 85-0477, Jan. 1985.

[30] Tagawa, M., Ohmae, N., Umeno, M., Yasukawa, A., Gotoh, K., and Tagawa, M., "Surface Characterization of Carbon Fibers Exposed to 5eV Energetic Atomic Oxygen Beam Studied by Wetting Force Measurements," *Japanese Journal of Applied Physics*, Vol. 30, No. 9A, 1991, pp. 2134–2138.

[31] Leger, L. J., Koontz, S. L., Visentine, T., and Cross, J. B., "Laboratory Investigations Involving High-Velocity Oxygen Atoms," *Proceedings of International Symposium on Spacecraft Materiarls and Space Environments* (Toulouse, France), Cepadues-editions, Sept. 1988, pp. 393–404.

[32] Matijasevic, V., Garwin, E. L., and Hammond, R. H., "Atomic Oxygen Detection by a Silver-coated Quartz Deposition Monitor," *Review of Scientific Instruments*, Vol. 61, No. 6, 1990, pp. 1747–1749.

[33] Deal, B. E., and Grove, A. S., "General Relationship for the Thermal Oxidation of Silicon," *Journal of Applied Physics*, Vol. 36 No. 12, 1965, pp. 3770–3778.

[34] Roberts, E. W., "Ultralow Friction Films of MoS$_2$ for Space Applications," *Thin Solid Films*, Vol. 181, No. 1, 1989, pp. 461–473.

[35] Ohmae, N., "Reactions of Atomic Oxygen with Solid Surfaces as Related to Spacetribology in Low Earth Orbit," *Proceedings of the 1st International Workshop on Microtribology* (Tokyo), Japanese Society of Tribologist, 1992, pp. 266–275.

[36] Cross, J. B., Martin, J. A., Pope, L. E., and Koontz, S. L., "Atomic Oxygen-MoS$_2$ Chemical Interactions," *Surface and Coating Technology*, Vol. 42, No. 1, 1990, pp. 41–48.

[37] Arita, M., Yasuda, Y., Kishi, K., Ohmae, N., and Shichi, Y., "Reactions Between Atomic Oxygen and MoS$_2$-based Solid Lubricants," *Proceedings of JAST Tribology Conference* (Tokyo), Japanese Society of Tribologist, 1992, pp. 405–408 (in Japanese).